M. van Haren *et al*, "A Frequency-Domain Approach for Enhanced Performance and Task Flexibility in Finite-Time ILC," published in *European Journal of Control*, 2024, uploaded June 21, 2024

A Frequency-Domain Approach for Enhanced Performance and Task Flexibility in Finite-Time ILC

Max van Haren[1], Kentaro Tsurumoto[2], Masahiro Mae[2],
Lennart Blanken[1,3], Wataru Ohnishi[2] and Tom Oomen[1,4]

***Abstract*— Iterative learning control (ILC) techniques are capable of improving the tracking performance of control systems that repeatedly perform similar tasks by utilizing data from past iterations. The aim of this paper is to achieve both the task flexibility enabled by ILC with basis functions and the performance of frequency-domain ILC, with an intuitive design procedure. The cost function of norm-optimal ILC is determined that recovers frequency-domain ILC, and consequently, the feedforward signal is parameterized in terms of basis functions and frequency-domain ILC. The resulting method has the performance and design procedure of frequency-domain ILC and the task flexibility of basis functions ILC, and are complimentary to each other. Validation on a benchmark example confirms the capabilities of the framework.**

I. Introduction

The increasing requirements for precision mechatronics result in a situation where both tracking performance and task flexibility, which is the ability to have high performance for different references, are important. Feedforward control is effective in compensating known disturbances for systems, leading to improved performance. Feedforward control is often based on models [1], which is generally achieved in industrial applications by means of basis functions feedforward control. In basis functions feedforward control, the feedforward signal is a linear combination of basis functions that relate to physical quantities, such as acceleration feedforward for the inertia [2–4]. Due to modeling and tuning inaccuracies, the increasing requirements for performance are generally not achieved.

This work is part of the research programme VIDI with project number 15698, which is (partly) financed by the Netherlands Organisation for Scientific Research (NWO). In addition, this research has received funding from the ECSEL Joint Undertaking under grant agreement 101007311 (IMOCO4.E). The Joint Undertaking receives support from the European Union Horizon 2020 research and innovation programme. Furthermore, it is partially funded by the joint JSPS-NWO funding programme *Research Network on Learning in Machines*, with grant numbers JPJSBP220234403 and 040.040.060. It is also partly supported by JSPS KAKENHI grant numbers 23H01431, and 24KJ0959.

[1]Max van Haren, Lennart Blanken and Tom Oomen are with the Control Systems Technology Section, Department of Mechanical Engineering, Eindhoven University of Technology, Eindhoven, The Netherlands, e-mail: m.j.v.haren@tue.nl.

[2] Kentaro Tsurumoto, Masahiro Mae and Wataru Ohnishi are with the department of Electrical Engineering and Information Systems, the University of Tokyo, Tokyo, Japan.

[3] Lennart Blanken is with Sioux Technologies, Eindhoven, The Netherlands.

[4]Tom Oomen is with the Delft Center for Systems and Control, Delft University of Technology, Delft, The Netherlands.

Iterative Learning Control (ILC) can improve tracking performance with respect to model based feedforward control [5], and hence, can fulfill the increasing requirements for performance. ILC utilizes information from past iterations to improve the tracking performance in the current iteration. For ILC to be industrially applicable, it is required that ILC

(R1) is task flexible;
(R2) has high tracking performance; and
(R3) has an intuitive design procedure.

In this paper, two types of ILC are considered, and are referred to as frequency-domain and norm-optimal ILC.

First, frequency-domain ILC uses infinite-time frequency-domain system representations to iteratively update the feedforward signal [6]. Frequency-domain ILC has the advantage that convergence can be verified and tuned using frequency response functions (FRFs), that are accurate and inexpensive to obtain [7]. As a result, frequency-domain ILC leads to an intuitive frequency-domain design procedure consisting of manual loop shaping and has high tracking performance. Frequency-domain ILC is typically implemented in finite-time, where convergence can still be analyzed [8]. However, conventional frequency-domain ILC is not directly capable of task flexibility, and hence, does not satisfy requirement R1.

Second, norm-optimal ILC utilizes a finite-time cost function to iteratively optimize the feedforward signal [9]. The main advantage of norm-optimal ILC is that the feedforward signal can be parameterized into basis functions, that enables task flexibility [10, 11]. However, if the basis functions are not sufficiently rich to describe the inverse system, the performance is significantly worse compared to frequency-domain ILC, and therefore does not achieve requirement R2.

Important developments have been made to combine the task flexibility of ILC with basis functions and the performance of frequency-domain ILC. In [12, 13], frequency-domain ILC is projected on basis functions, resulting in task flexibility, but reducing tracking performance. Furthermore, in [14], frequency-domain ILC is combined with ILC with basis functions using a sequential optimization problem, that results in the performance of frequency-domain ILC and the task flexibility of ILC with basis functions. However, the approach results in an unintuitive design procedure, not satisfying requirement R3.

Although ILC methods with high performance and task flexibility are investigated, a method that achieves both high

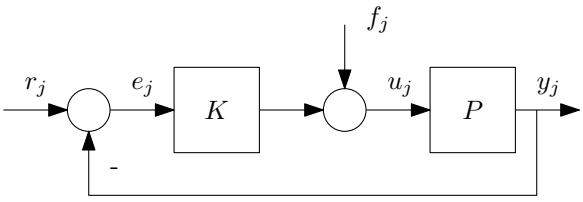

Fig. 1: Control structure considered.

performance and task flexibility, with an intuitive design procedure, is currently lacking. In this paper, high performance (R2) is achieved by deliberately overparameterizing the feedforward signal in a low number of basis functions to accomplish task flexibility (R1). Additionally, a complementary signal is optimized via an intuitive frequency-domain ILC design (R3). The key contributions in this paper include the following.

(C1) Determining the equivalent norm-optimal finite-time representation of frequency-domain ILC by specific choice of weighting matrices, that enables intuitive tuning in the frequency-domain (R3) (Section III-A).

(C2) Achieving both task flexibility (R1) and high performance (R2) by exploiting an overparameterized feedforward signal, building upon C1 (Section III-B).

(C3) Validation of the framework on an example (Section IV).

Notation: Let $\mathcal{H}(z)$ denote a discrete-time, Linear Time-Invariant (LTI), single-input, single-output system. The frequency response function of $\mathcal{H}(z)$ is obtained by substituting $z = e^{j\omega}\ \forall \omega \in [0, 2\pi)$, and is denoted by $\mathcal{H}(e^{j\omega})$.

Signals are of length N. Vectors are denoted as lowercase letters and matrices as uppercase letters, e.g., x and X. The z-transform of signal $x(k)$ is $\mathcal{X}(z) = \sum_{k=0}^{\infty} x(k)z^{-1}$. Let $h(k)\ \forall k \in \mathbb{Z}$ be the impulse response coefficients of $\mathcal{H}(z)$, with infinite impulse response $y(k) = \sum_{\tau=-\infty}^{\infty} h(\tau)u(k-\tau)$. Let $u(k) = 0$ for $k < 0$ and $k \geq N$ to obtain the finite-time convolution

$$\underbrace{\begin{bmatrix} y(0) \\ y(1) \\ \vdots \\ y(N-1) \end{bmatrix}}_{y} = \underbrace{\begin{bmatrix} h(0) & h(-1) & \cdots & h(-N+1) \\ h(1) & h(0) & \cdots & h(-N+2) \\ \vdots & \vdots & \ddots & h(-1) \\ h(N-1) & h(N-2) & \cdots & h(0) \end{bmatrix}}_{H} \underbrace{\begin{bmatrix} u(0) \\ u(1) \\ \vdots \\ u(N-1) \end{bmatrix}}_{u},$$

with $y, u \in \mathbb{R}^N$ and $H \in \mathbb{R}^{N \times N}$ is the finite-time convolution matrix corresponding to $\mathcal{H}(z)$.

II. Problem Formulation

In this section, the problem that is dealt with in this paper is formulated. First, the problem setup is presented. Second, the different classes of ILC considered in this paper are described. Finally, the problem that is addressed in this paper is defined.

A. Problem Setup

The control structure is seen in Fig. 1. The LTI system P is stabilized by LTI feedback controller K. The finite-time reference signal $r_j \in \mathbb{R}^N$ can be trial varying. The goal is to reduce the reference induced error signal $e_j \in \mathbb{R}^N$ over multiple trials j with the trial-varying feedforward signal $f_j \in \mathbb{R}^N$.

B. Classes of ILC

In this section, the three considered classes of ILC, that is norm-optimal ILC, ILC with basis functions and frequency-domain ILC, are presented.

1) Norm-Optimal ILC: Norm-optimal ILC is a type of ILC that minimizes a finite-time cost function, typically

$$\min_{f_{j+1}^{NO}} \|\hat{e}_{j+1}\|_{W_e}^2 + \left\|f_{j+1}^{NO}\right\|_{W_f}^2 + \left\|f_{j+1}^{NO} - f_j^{NO}\right\|_{W_{\Delta f}}^2, \quad (1)$$

where $\|x\|_W^2 = x^\top W x$, W_e, W_f and $W_{\Delta f}$ are symmetric positive (semi)definite weighting matrices [9], $\hat{e}_{j+1} = e_j - \hat{J}\left(f_{j+1}^{NO} - f_j^{NO}\right)$, and finite-time convolution matrix $\hat{J} = \hat{P}\left(I + K\hat{P}\right)^{-1}$, with convolution matrix $\widehat{P} \in \mathbb{R}^{N \times N}$ representing model $\widehat{\mathcal{P}}$ of system $\mathcal{P}$, and identity matrix $I \in \mathbb{R}^{N \times N}$. The cost function in (1) is quadratic in the optimization variables f_{j+1}^{NO}, and hence, has a minimizer that is analytically computed as

$$f_{j+1}^{NO} = Q^{NO} f_j + L^{NO} e_j, \quad (2)$$

with norm-optimal ILC robustness and learning matrices Q^{NO} and L^{NO}.

2) ILC with Basis Functions: ILC with basis functions achieves reference flexibility by minimizing a cost function and parameterizing the feedforward signal in basis functions as

$$f_j = \psi \theta_j, \quad (3)$$

with feedforward parameters $\theta_j \in \mathbb{R}^{n_\theta \times 1}$ and basis functions $\psi \in \mathbb{R}^{N \times n_\theta}$. For ILC with basis functions, the cost function

$$\min_{\theta_{j+1}} \|\hat{e}_{j+1}\|_{W_e}^2 + \|f_{j+1}\|_{W_f}^2 + \|f_{j+1} - f_j\|_{W_{\Delta f}}^2, \quad (4)$$

is minimized. Similarly to norm-optimal ILC in (2), the optimal solution to (4) is of the form

$$\theta_{j+1} = Q^{BF} \theta_j + L^{BF} e_j, \quad (5)$$

with basis functions robustness and learning matrices Q^{BF} and L^{BF}.

3) Frequency-Domain ILC: Frequency-domain ILC iteratively improves the tracking performance by utilizing infinite-time frequency-domain representations. Frequency-domain ILC is designed by the infinite-time update law

$$\mathcal{F}_{j+1}^f(z) = \mathcal{Q}^f(z)(\mathcal{F}_j^f(z) + \alpha \mathcal{L}^f(z)\mathcal{E}_j(z)), \quad (6)$$

with $\mathcal{Q}^f$ the robustness filter, that is used to enforce convergence and filter out unwanted effects, $\mathcal{L}^f$ the learning filter and α the learning gain. Frequency-domain ILC is implemented in finite-time as [8]

$$f_{j+1}^f = Q^f(f_j^f + \alpha L^f e_j), \quad (7)$$

with finite-time convolution matrices Q^f and L^f, corresponding to $\mathcal{Q}^f(z)$ and $\mathcal{L}^f(z)$.

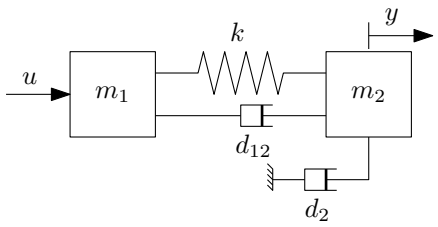

Fig. 2: System that is used for validation. The system is discretized with zero-order hold, and has one sample delay.

C. Problem Definition

The aforementioned classes of ILC have several design problems and limitations, and are as follows.

- For norm-optimal ILC, it is highly complex to robustly choose the weighting matrices, see for example [15, 16], and $W = wI$ severely limits performance. Furthermore, norm-optimal ILC does not have task flexibility.
- ILC with basis functions reduces performance if ψ does not accurately describe the inverse system P^{-1} [13, 17].
- Frequency-domain ILC does have an intuitive design procedure consisting of manual loop-shaping [5, 13] and results in high performance, but conventionally does not have task flexibility.

In Example 1, the limited performance of norm-optimal ILC with identity weighting matrices and model uncertainty is illustrated, since robust monotonic convergence is difficult to achieve.

Example 1: A simulation study illustrates that frequency-domain ILC performs better than norm-optimal ILC for an inaccurate model and identity weighting matrices. The system is a mass-spring-damper as seen in Fig. 2,where further elaboration is provided in Section IV. The error 2-norm during 300 trials of norm-optimal and frequency-domain ILC is shown in Fig. 3a, and the maximum error 2-norm during these trials and the steady state error 2-norm $\|e_\infty\|_2$ are shown in Fig. 3b. The results in Fig. 3 illustrate that for norm-optimal ILC to reduce the steady-state error $\|e_\infty\|_2$ beyond frequency-domain ILC, it first increases the maximum error 2-norm $\max_j \left(\|e_j\|_2\right)$ at least a factor $3 \cdot 10^6$ due to non-monotonic convergence, which is unacceptable in industrial applications.

Hence, the problem addressed in this paper is to develop an ILC algorithm that simultaneously satisfies all three requirements for industrial applicability of ILC, that combines the advantages of current ILC techniques.

III. Method

In this section, the developed method is presented. The overparameterized feedforward signal

$$f_j = \Psi\Theta_j = \begin{bmatrix}\psi & I_N\end{bmatrix}\begin{bmatrix}\theta_j \\ f_j^f\end{bmatrix} = \psi\theta_j + f_j^f, \tag{8}$$

that consists of basis functions and frequency-domain ILC, is exploited to achieve both task flexibility and high performance, leading to (R1) and (R2). Frequency-domain ILC is used since it has better performance than norm-optimal ILC for inaccurate models, as shown in Section II, and due to its intuitive design procedure (R3).

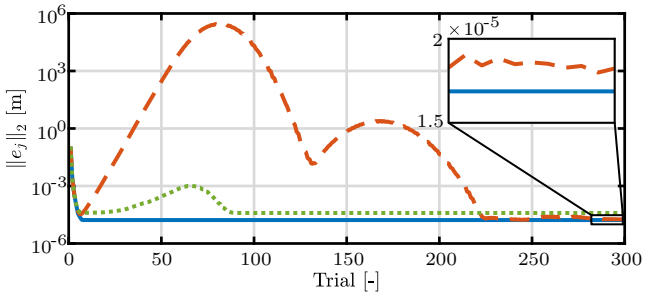

(a) Error 2-norm for frequency-domain ILC (—) and norm-optimal ILC with $W_f = 1.39{\cdot}10^{-8}I$ (····) and $W_f = 5.2{\cdot}10^{-9}I$ (- -).

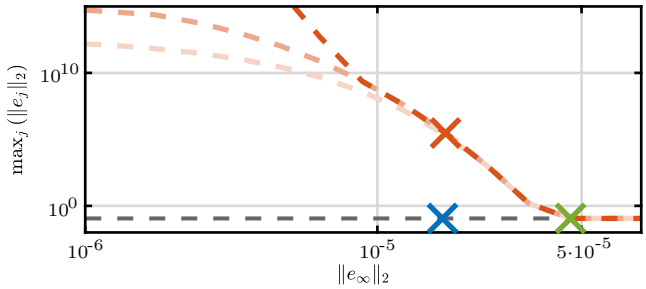

(b) Steady-state and maximum error 2-norm for norm-optimal ILC with $W_f = w_f I \,\forall\, w_f \in [10^{-14}, 10^{-7}]$ after 75 (···), 150 (- -) and 300 (- -) trials, $W_f = 5.2 \cdot 10^{-9}I$ (×) and $W_f = 1.9 \cdot 10^{-8}I$ (×) correspond to Fig. 3a, frequency-domain ILC (×), and maximum error 2-norm for $f_j = 0$ (- -).

Fig. 3: Illustration that norm-optimal ILC with $W_e = I$ and $W_{\Delta f} = 0$ converges slowly and non-monotonically for inaccurate models.

First, the norm-optimal description of frequency-domain ILC is determined, such that second, the overparameterized feedforward signal in (8) consisting of frequency-domain and ILC with basis functions can be jointly optimized. Finally, a procedure summarizes the developed method.

A. Norm-Optimal Representation of Frequency-Domain ILC

In this section, it is shown that the finite-time implementation of frequency-domain ILC in (7) is equivalent to (1) for a very specific choice of weighting matrices W_e, W_f and $W_{\Delta f}$. First, the finite-time frequency-domain ILC update is written using the cost function

$$\min_{f_{j+1}^f} \|\hat{e}_{j+1}\|^2_{W_e^f} + \left\|f_{j+1}^f\right\|^2_{W_f^f} + \left\|f_{j+1}^f - f_j^f\right\|^2_{W_{\Delta f}^f}, \tag{9}$$

that is minimized by

$$\begin{aligned} f_{j+1}^f =& (\hat{J}^\top W_e^f \hat{J} + W_f^f + W_{\Delta f}^f)^{-1}\left(\hat{J}^\top W_e^f \hat{J} + W_{\Delta f}^f\right) f_j^f \\ &+ (\hat{J}^\top W_e^f \hat{J} + W_f^f + W_{\Delta f}^f)^{-1}\hat{J}^\top W_e^f e_j \\ =& Q^f(f_j^f + \alpha L^f e_j), \end{aligned} \tag{10}$$

where the last identity is found by substituting f_{j+1}^f from the finite-time update law of frequency-domain ILC in (7). The

contributions of f_j^f and e_j in (10) are separated to achieve

$$Q^f = (\hat{J}^\top W_e^f \hat{J} + W_f^f + W_{\Delta f}^f)^{-1} \left(\hat{J}^\top W_e^f \hat{J} + W_{\Delta f}^f\right), \tag{11}$$

$$\alpha Q^f L^f = (\hat{J}^\top W_e^f \hat{J} + W_f^f + W_{\Delta f}^f)^{-1} \hat{J}^\top W_e^f. \tag{12}$$

From (11), W_f^f is derived as

$$W_f^f = \left(\hat{J}^\top W_e^f \hat{J} + W_{\Delta f}^f\right) \left(\left(Q^f\right)^{-1} - I\right). \tag{13}$$

Because W_f^f must be symmetric and positive semidefinite, but the product of two symmetric matrices is not necessarily symmetric, $\left(\hat{J}^\top W_e^f \hat{J} + W_{\Delta f}^f\right)$ in (13) is chosen

$$\left(\hat{J}^\top W_e^f \hat{J} + W_{\Delta f}^f\right) = I. \tag{14}$$

By substituting (14) and W_f^f from (13) into (12), the following identity is found

$$\alpha Q^f L^f = Q^f \hat{J}^\top W_e^f, \tag{15}$$

leading to the main result in this section in Theorem 1.

Theorem 1: Let $\hat{J}$ be invertible and $L^f = \hat{J}^{-1}$, then the minimizer of the cost function in (9) with

$$W_e^f = \alpha \hat{J}^{-\top} L^f, \tag{16a}$$

$$W_f^f = \left(Q^f\right)^{-1} - I, \tag{16b}$$

$$W_{\Delta f}^f = (1-\alpha) I, \tag{16c}$$

is equal to finite-time frequency-domain ILC in (7).

Proof: Straightforward manipulation of (15) lead to W_e in (16a). Substituting (14) into (13) leads to W_f in (16b). Finally, the resulting W_e in (16a) is substituted into (14) to result in $W_{\Delta f}$ in (16c). ∎

Remark 1: The conditions that $\hat{J}$ is invertible and $L^f = \hat{J}^{-1}$ in Theorem 1 are not restrictive, since the weighting matrix W_e^f can be approximated as the symmetric matrix

$$W_e^f = \alpha {L^f}^\top L^f, \tag{17}$$

since L^f is similar to J^{-1}, and is shown in Section IV-A.

Assumption 1: To ensure that W_f^f in (16b) is symmetric, there is assumed that the robustness filter is designed with zero-phase, i.e., $\mathcal{Q}^f(z) = \mathcal{Q}_1^f(\frac{1}{z})\mathcal{Q}_1^f(z)$ [9].

To summarize, finite-time frequency-domain ILC in (7) is recovered by specifically choosing the weighting matrices (16a), (16b) and (16c) and optimizing (9), resulting in an intuitive frequency-domain design procedure (R3) for norm-optimal ILC. In the next section, the norm-optimal description of frequency-domain ILC is used when overparameterizing the feedforward signal.

B. Inclusion of Basis-Function in Frequency-Domain ILC

In this section, both task flexibility and high performance are achieved by deliberately overparameterizing the feedforward in terms of basis functions and frequency-domain ILC by utilizing the norm-optimal representation of finite-time frequency-domain ILC. The cost function in (9) is adjusted by utilizing the overparameterized feedforward signal in (8) and preserving the weighting W_f^f and $W_{\Delta f}^f$ exclusively on the frequency-domain component as

$$\begin{aligned}\min_{\Theta_{j+1}} V(\Theta_{j+1}) = \min_{\Theta_{j+1}} \|\hat{e}_{j+1}\|_{W_e^f}^2 + \|\Theta_{j+1}\|_{W_{\theta,f}}^2 \\ + \|\Theta_{j+1} - \Theta_j\|_{W_\Delta}^2\end{aligned} \tag{18}$$

with

$$W_{\theta,f} = \begin{bmatrix} W_\theta & 0 \\ 0 & W_f^f \end{bmatrix}, \quad W_\Delta = \begin{bmatrix} W_{\Delta\theta} & 0 \\ 0 & W_{\Delta f}^f \end{bmatrix}, \tag{19}$$

where $W_\theta, W_{\Delta\theta} \in \mathbb{R}^{n_\theta \times n_\theta}$ are the weighting matrices on the feedforward parameters θ, that are typically chosen as $W_\theta = w_\theta \psi^\top \psi$ and $W_{\Delta\theta} = w_{\Delta\theta} \psi^\top \psi$, resulting in equivalent weighting as conventional ILC with basis functions. The minimizer of (18) is given by

$$\begin{aligned}\Theta_{j+1} = &\left(\Psi^\top \hat{J}^\top W_e^f \hat{J} \Psi + W_{\theta,f} + W_\Delta\right)^{-1} \\ &\cdot \left(\left(\Psi^\top \hat{J}^\top W_e^f \hat{J} \Psi + W_\Delta\right)\Theta_j + \Psi^\top \hat{J}^\top W_e^f e_j\right).\end{aligned} \tag{20}$$

Remark 2: If the weighting on θ is chosen sufficiently small $W_\theta << W_f^f$, the parameterization (8) consisting of frequency-domain and ILC with basis functions is naturally complimentary and the parameterization will assign as much information in the basis functions feedforward signal as possible. Additionally, a targeted regularization on the frequency-domain component can be done by using the image of ψ, similarly to [18],

$$\min_{\Theta_{j+1}} V(\Theta_{j+1}) + \lambda \left\| \begin{bmatrix} 0 & U_1 \end{bmatrix} \Theta_{j+1} \right\|_2^2,$$

with singular value decomposition

$$\psi = \begin{bmatrix} U_1 & U_2 \end{bmatrix} \begin{bmatrix} \Sigma & 0 \\ 0 & 0 \end{bmatrix} \begin{bmatrix} V_1^\top \\ V_2^\top \end{bmatrix}.$$

C. Procedure

In this section, the developed method for achieving task flexibility, high performance and an intuitive design procedure by combining frequency-domain ILC with basis function ILC is summarized in Procedure 1.

IV. Simulation Example

In this section, the developed method is validated and compared with frequency-domain and ILC with basis functions. First, the validation setup is shown, including the system and model, the reference signals and the ILC designs. Second, the norm-optimal equivalent description of frequency-domain ILC is validated. Finally, the developed method with basis functions is validated and compared for a trial-varying reference signal.

A. Simulation Setup and Approach

A two-mass-spring-damper system with one sample delay and a sampling time of 1 ms, with inaccurate model, is simulated to validate the developed ILC technique. The mass-spring-damper system represents the dominant dynamics of mechatronic systems [3, 4], and is for example an actuator

Procedure 1: (*Norm-optimal frequency-domain ILC with basis functions*)

1) Design learning filter $\mathcal{L}^f(z)$, α and zero-phase robustness filter $\mathcal{Q}^f(z)$ as in frequency-domain ILC.
2) Derive L^f and Q^f, that are the finite-time convolution matrices of $\mathcal{L}^f(z)$ and $\mathcal{Q}^f(z)$.
3) Choose the basis functions ψ in (8).
4) Compute equivalent norm-optimal weighting matrices W_e^f, W_f^f and $W_{\Delta f}^f$ using (16a), (16b) and (16c).
   a) If W_e is non-symmetrical, follow Remark 1.
5) Initialize Θ_1, e.g., as $\Theta_1 = 0$.
6) For $j \in \{1, 2, 3, \ldots, N_{trials}\}$.
   a) Calculate $f_j = \Psi\Theta_j$ in (8).
   b) Apply f_j to closed-loop system and record e_j.
   c) Calculate Θ_{j+1} using (20).

TABLE I: Parameters used for the system seen in Fig. 2 for the true system and model.

Parameter	True	Model	Unit
m_1	0.072	0.09	[kg]
m_2	0.01	0.006	[kg]
k	1000	1800	[N/m]
d_2	0.031	0	[Ns/m]
d_{12}	1	0.915	[Ns/m]

with a flexible coupling and mass attached. The system is seen in Fig. 2, and the parameters of the true system $\mathcal{P}(z)$ and the model $\widehat{\mathcal{P}}(z)$ are seen in Table I, and are given by

$$\mathcal{P}(z) = 10^{-7} \cdot \frac{2.80z^{-2} + 12.4z^{-3} - 0.65z^{-4} - 1.58z^{-5}}{1 - 3.78z^{-1} + 5.46z^{-2} - 3.56z^{-3} + 0.89z^{-4}},$$
$$\widehat{\mathcal{P}}(z) = 10^{-7} \cdot \frac{4.00z^{-2} + 21.4z^{-3} + 5.85z^{-4} - 1.25z^{-5}}{1 - 3.56z^{-1} + 4.98z^{-2} - 3.26z^{-3} + 0.85z^{-4}}. \quad (21)$$

The FRFs of $\mathcal{P}(e^{j\omega})$ and $\widehat{\mathcal{P}}(e^{j\omega})$ are seen in Fig. 4. Additionally, the FRF of the true system $\mathcal{P}(e^{j\omega})$ is available for stability analysis, but not for the design of learning filters. The feedback controller is a lead filter and a first-order low-pass filter, that achieves a closed-loop bandwidth of 10 Hz

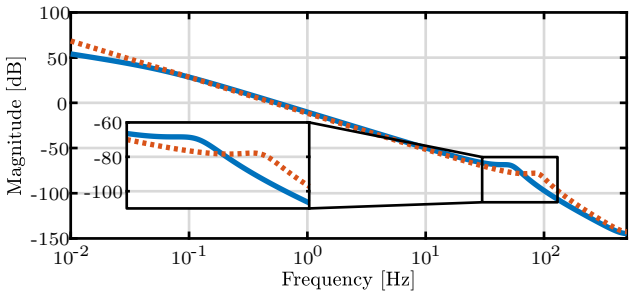

Fig. 4: FRF of the system $\mathcal{P}(e^{j\omega})$ (—) and of the model available for ILC $\widehat{\mathcal{P}}(e^{j\omega})$ (···).

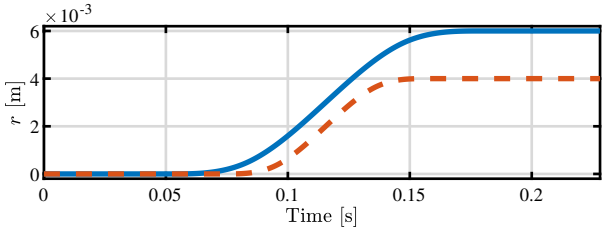

Fig. 5: The first (—) and second (- - -) reference signals that are used during validation.

with sufficient robustness margins, and is given by

$$\mathcal{K}(z) = \frac{108.6 + 112.9z^{-1} - 100z^{-2} - 104.3z^{-3}}{1 - 0.65z^{-1} - 0.95z^{-2} + 0.70z^{-3}}. \quad (22)$$

The learning filter $\mathcal{L}^f(z)$ is designed by approximating the inverse process sensitivity using ZPETC [19]. The robustness filter $\mathcal{Q}^f(z)$ is a zero-phase second order Butterworth lowpass filter with a cutoff frequency of 40 Hz, that was manually tuned to achieve convergence according to

$$\left|\mathcal{Q}^f(e^{j\omega})(1 - \alpha\mathcal{J}(e^{j\omega})\mathcal{L}^f(e^{j\omega}))\right| < 1, \quad \forall\omega \in [0, 2\pi]. \quad (23)$$

Two fourth-order polynomial reference signals are designed using the approach in [3] with $N = 229$ samples and are seen in Fig. 5. Following 10 consecutive trials with the first reference signal, it is then switched to the second reference signal for another 10 consecutive trials.

a) Basis Function Design: The basis functions ψ are based on the inverse model of $\widehat{\mathcal{P}}(z)$ and are chosen as

$$\psi = \begin{bmatrix} \ddot{r} & \ddddot{r} \end{bmatrix}, \quad (24)$$

where the derivatives of the reference signal are readily available by design of the reference signal. W_θ and $W_{\Delta\theta}$ in (19) are chosen as 0, since no additional robustness is necessary.

b) Recovering Norm-Optimal Formulation of Frequency-Domain ILC: W_f^f and $W_{\Delta f}^f$ are calculated using respectively (16b) and (16c), resulting in $W_{\Delta f}^f = 0$ since $\alpha = 1$. W_e^f is computed using (17), since $L^f \neq \hat{J}^{-1}$ due to the use of ZPETC, as indicated in Remark 1. A surface plot of the weighting matrix W_f^f is seen in Fig. 6. Frequency-domain ILC and its norm-optimal equivalent achieve the same tracking error for every trial, where the error signal during trial 5 and 10 are shown in Fig. 7, validating their equivalence.

B. Validation Results

The error 2-norm and signal for 20 trials of ILC are seen in Fig. 8 and Fig. 9. The plant estimate using the basis function feedforward filter is seen in Fig. 10. The following observations are made.

- Fig. 8 shows frequency-domain ILC is converged at trials 10 and 20. However, its error 2-norm significantly increases at trial 11, showing that it lacks task flexibility.

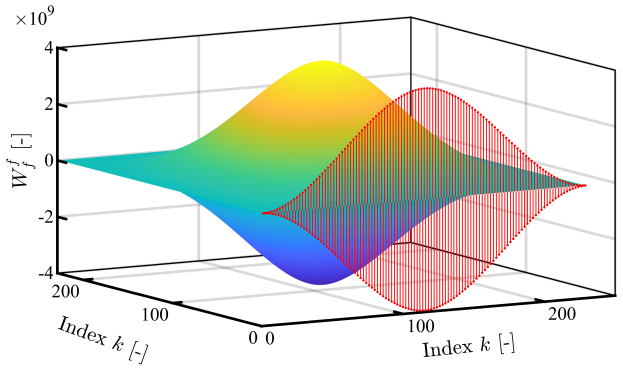

Fig. 6: Surface plot of the weighting matrix W_f^f (■), with cross section of the central values (—•—), that if used in the norm-optimal cost function (1) results in the frequency-domain ILC update.

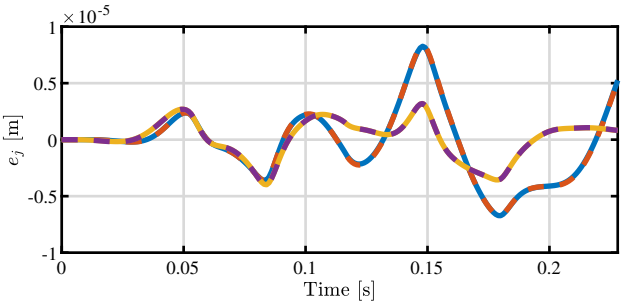

Fig. 7: Tracking performance after 5 trials of ILC for frequency-domain ILC (—) and norm-optimal equivalent (- -) and after 10 trials for frequency-domain ILC (—) and norm-optimal equivalent (- -) using the first reference signal, showing the same error signal.

- Though ILC with basis functions enables reference flexibility as seen in Fig. 8, its higher error 2-norm compared to the other methods stems from lacking $\dot{r}$ in its basis function ψ to compensate the viscous friction d_2.
- The error 2-norm in Fig. 8 and the time-domain error signal for trial 20 in Fig. 9 demonstrate the developed approach's superior performance against both basis function and frequency-domain ILC. It surpasses basis functions ILC by compensating damping d_2 with the frequency-domain component, which is lacking in the basis function ψ. The developed approach outperforms frequency-domain ILC by capturing high-frequency effects with ψ, that for frequency-domain ILC is filtered out by robustness filter $\mathcal{Q}^f(z)$.
- Similar error 2-norm to ILC with basis functions under reference change illustrates the method's task flexibility.
- From Fig. 10 it becomes clear that the basis functions feedforward parameters θ_j are estimated consistently with the inverse model, which is enabled since $W_\theta = 0 << W_f^f$ as described in Remark 2.

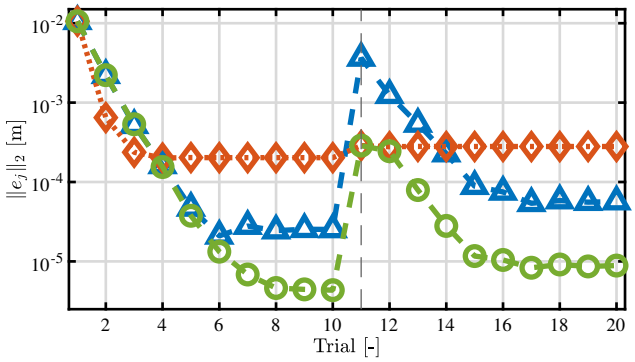

Fig. 8: Error 2-norm for 20 trials of frequency-domain ILC (—▲—), basis function ILC (—♦—) and developed combined frequency-domain and basis function ILC (—○—). At trial 11, the reference signal is changed (- -).

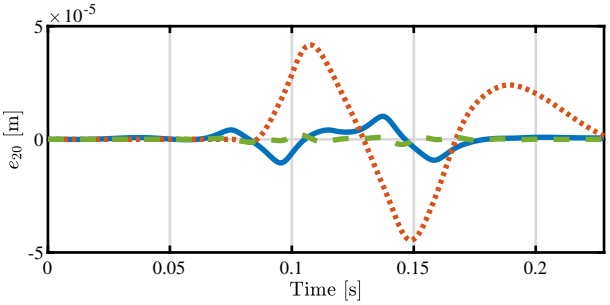

Fig. 9: Tracking error after 20 trials e_{20} of frequency-domain ILC (—), basis function ILC (···) and developed combined frequency-domain and basis function ILC (- -).

V. Conclusions

In this paper, both task flexibility and performance are achieved through the use of an overparameterized feedforward signal consisting of frequency-domain and basis functions ILC. The finite-time norm-optimal representation of frequency-domain ILC is derived, that is consequently used in overparameterizing the feedforward signal. The basis functions and frequency-domain ILC components are complimentary by appropriately regularizing the frequency-domain component. An example validates the equivalent norm-optimal representation, and by exploiting the overparameterized feedforward signal, the performance is significantly increased. Hence, the developed method is a key enabler for improving performance and task flexibility in control.

Ongoing research focuses on rigorously validating the method through experimental testing on a real-world setup, in addition to computationally efficient implementations and validating robustness of the developed approach.

References

[1] J. Butterworth, L. Pao, and D. Abramovitch, "Analysis and comparison of three discrete-time feedforward model-inverse control techniques for nonminimum-phase systems," *Mechatronics*, vol. 22 (5), 2012.

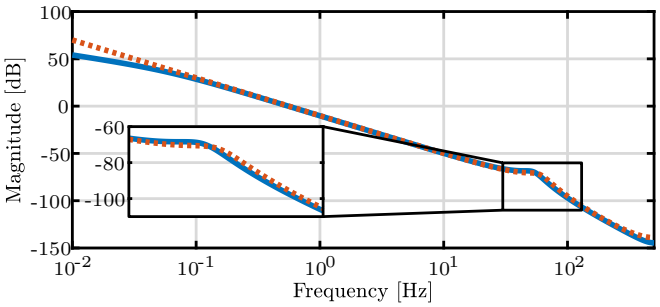

Fig. 10: FRFs of system $\mathcal{P}(e^{j\omega})$ (—) and of estimate using the inverse basis function feedforward filter $\mathcal{F}_{BF}^{-1}(e^{j\omega}, \theta_j)$ (···), with finite-time representation $F_{BF}(\theta_j)r = \psi\theta_j$.

[2] M. Boerlage, R. Tousain, and M. Steinbuch, "Jerk derivative feedforward control for motion systems," in *Am. Control Conf.*, vol. 5 (1), 2004.

[3] P. Lambrechts, M. Boerlage, and M. Steinbuch, "Trajectory planning and feedforward design for electromechanical motion systems," *Control Eng. Pract.*, vol. 13 (2), 2005.

[4] T. Oomen, "Control for Precision Mechatronics," in *Encycl. Syst. Control*, London: Springer London, 2020, pp. 1–10.

[5] D.A. Bristow ; M. Tharayil ; A.G Alleyne., D. A. Bristow, and M. Tharayil, "A survey of iterative learning control," *IEEE Control Syst.*, vol. 26 (3), 2006.

[6] S. Arimoto, S. Kawamura, and F. Miyazaki, "Bettering operation of Robots by learning," *J. Robot. Syst.*, vol. 1 (2), 1984.

[7] R. Pintelon and J. Schoukens, *System Identification: A Frequency Domain Approach*. John Wiley & Sons, 2012.

[8] M. Norrlöf and S. Gunnarsson, "Time and frequency domain convergence properties in iterative learning control," *Int. J. Control*, vol. 75 (14), 2002.

[9] S. Gunnarsson and M. Norrlöf, "On the design of ILC algorithms using optimization," *Automatica*, vol. 37 (12), 2001.

[10] M. Phan and J. Frueh, "Learning control for trajectory tracking using basis functions," in *Proc. 35th IEEE Conf. Decis. Control*, vol. 3, 1996.

[11] J. van de Wijdeven and O. Bosgra, "Using basis functions in iterative learning control: analysis and design theory," *Int. J. Control*, vol. 83 (4), 2010.

[12] S. Mishra and M. Tomizuka, "Projection-Based Iterative Learning Control for Wafer Scanner Systems," *IEEE/ASME Trans. Mechatronics*, vol. 14 (3), 2009.

[13] F. Boeren, A. Bareja, T. Kok, and T. Oomen, "Frequency-Domain ILC Approach for Repeating and Varying Tasks: With Application to Semiconductor Bonding Equipment," *IEEE/ASME Trans. Mechatronics*, vol. 21 (6), 2016.

[14] K. Tsurumoto, W. Ohnishi, and T. Koseki, "Task Flexible and High Performance ILC: Preliminary Analysis of Combining a Basis Function and Frequency Domain Design Approach," in *IFAC World Congr.*, 2023.

[15] J. X. Xu and Y. Tan, "On the robust optimal design and convergence speed analysis of iterative learning control approaches," *Automatica*, vol. 15 (1), 2002.

[16] B. D. Gorinevsky, "Loop shaping for iterative control of batch processes," *IEEE Control Syst.*, vol. 22 (6), 2002.

[17] J. van Zundert, J. Bolder, and T. Oomen, "Optimality and flexibility in Iterative Learning Control for varying tasks," *Automatica*, vol. 67, 2016.

[18] J. Kon, N. de Vos, D. Bruijnen, J. van de Wijdeven, M. Heertjes, and T. Oomen, "Learning for Precision Motion of an Interventional X-ray System: Add-on Physics-Guided Neural Network Feedforward Control," in *22nd IFAC World Congr.*, 2023.

[19] M. Tomizuka, "Zero Phase Error Tracking Algorithm for Digital Control," *ASME. J. Dyn. Sys., Meas., Control*, vol. 109 (1), 1987.